Hydrothermally Treated Banana Empty Fruit Bunch Fiber Activated Carbon for Pb(II) and Zn(II) Removal

Ganiyu Abimbola Adebisi, Zaira Zaman Chowdhury,* Sharifah Bee Abd Hamid, and Eaqub Ali

Activated carbon was produced by chemical activation of hydrothermally carbonized (HTC) banana empty fruit bunch (BEFB), using phosphoric acid (H_3PO_4) as the activating agent. The activation process was optimized using a Box-Behnken factorial design (BBD), with an outcome of 17 different experiments under the predefined conditions. Three different parameters (activation temperature (x_1), activation time (x_2), and the concentration of activating acid (x_3)) were analyzed with respect to their influence on maximum adsorption percentage for divalent cations, Pb(II) (Y_1) and Zn(II) (Y_2), and carbon yield (Y_3). All process parameters had strong positive effects on adsorption capacity up to a certain limit. The specific surface area of the hydrochar (HTC) was enhanced substantially after the activation process. Scanning electron microscopy (SEM) revealed that the morphology of the BEFB-based char changed noticeably after the acid impregnation and activation process. The Langmuir maximum monolayer adsorption capacity for Pb (II) and Zn (II) cations was 74.62 mg/g and 77.51 mg/g, respectively. Equilibrium isotherm data were in agreement with the Langmuir model. Thermodynamic characterization revealed that the equilibrium system was endothermic and spontaneous.

INTRODUCTION

The global demand for activated carbon (AC) has prompted research investigating new precursors and production methods to obtain micro- and nano-structured carbon for versatile applications. The AC is manufactured by chemical or physical activation methods; frequently, lignocellulosic biomass residues are the starting materials (Chowdhury *et al.* 2013). During physical activation, the biomass sample is first pyrolyzed (> 500 °C) and treated with an activating agent (air, carbon dioxide, and water or steam) at a high temperature (700 to 900 °C). For chemical activation, the residues are impregnated with chemicals and then pyrolyzed at moderate to high temperatures. Overall, the process can be made more energy-efficient by modifying the carbonization step, which decreases the production costs (Roman *et al.* 2013). The combination of hydrothermal and chemical activation methods functionalizes the carbon with tunable surface chemistry (Roman *et al.* 2013).

A hydrothermal carbonization technique (HTC) has been used to produce carbonaceous char (Titirici *et al.* 2007a; Sevilla and Fuertes 2009). During hydrothermal pretreatment, a lignocellulosic residue is carbonized under a mild temperature range (150 to 250 °C) and self-generated pressures using deionized water as the "green" solvent.

The HTC process is very popular because of its simplicity in design, cost savings, and energy efficiency. Furthermore, it is a "green method," as it does not employ organic solvents, corrosive catalysts, or surfactants (Titirici *et al.* 2007b). During hydrothermal carbonization, linkages between the carbohydrate-rich fractions, *i.e.*, cellulose and hemicellulose, are broken and dissolved in water. Consequently, a complex aldol reaction, cycloaddition, and condensation process yield carbonaceous hydrochar. The liquid phase contains some sugars or lignin-based oligomers, which can be used to extract value-added products including bioplastics and biofuels. Overall, the process is energy efficient and uses milder conditions than classical pyrolysis. Moreover, it does not require drying of the raw biomass, and the process is exothermic, releasing heat that contributes one-third of the energy needed for the complete carbonization process (Roman *et al.* 2013). In addition, the process does not produce toxic gases and tar-like pyrolysis (Xiu *et al.* 2010). Hydrothermal carbonization of biomass can provide a new type of starting material to produce activated carbon. HTC char is chemically similar to peat and lignite and can be further transformed to functional activated carbon (Hao *et al.* 2014). HTC char has good self-binding properties, which is advantageous for pelletisation (Amaya *et al.* 2007). Finally, the HTC process does not require gas flow, making it economically feasible, and most of the generated carbon is confined to the carbonaceous hydrochar (Amaaya *et al.* 2007). Hydrochar prepared from biomass residues has certain porosity, with special morphological features like nano-spheres or nano-fibers (Titirici *et al.* 2008). Its surface functional groups are hydrophilic. Thus, hydrochar can be the precursor to activated carbon with the appropriate surface chemistry to adsorb heavy metals from water. The activation of HTC materials with different activating agents and the physiochemical characteristics of the porous activated carbon have not been thoroughly studied. HTC contains a cross-linked polyfuranic structure, and the connections between the furan rings are composed of an aliphatic chain with oxygen groups. A small fraction of aromatic arene-like structures are observed after processing the biomass at 180 °C. With increasing temperature, the aromaticity increases, but the aliphatic and oxygen-containing groups decrease (Falco *et al.* 2013). This effect was attributed to oxygenated linking groups inside the final carbon matrix, which contains many reactive functional groups and hydrophilic structures than the pyrolyzed material.

In this report, hydrochar prepared from banana empty fruit bunch (BEFB) was used to prepare activated carbon for the removal of Pb(II) and Zn(II) cations from wastewater. The activation parameters were optimized with a 3-level factorial design based on Box-Behnken (BBD) modeling, which concurrently investigates the interdependence of several factors (Baskan and Pala 2010). The experimental variables are typically varied between two levels. This approach is systematic and describes nonlinear dependencies for a particular variable and interactions between variables. Compared with other response surface designs, BBD is slightly more efficient than the central composite design but much more efficient than the three-level full factorial designs (Ferreira *et al.* 2007). In this research, BBD design was applied to the parameters of temperature, time, and H_3PO_4 acid concentration for the activation of HTC obtained from BEFB. The resultant AC was used to absorb Pb(II) and Zn(II) from wastewater. The experimental data was analyzed using Langmuir, Freundlich, and Temkin Isotherm models. Thermodynamic characterization of the system determined the Gibb's Free energy ($\Delta G°$), enthalpy ($\Delta H°$), and entropy ($\Delta S°$) values.

EXPERIMENTAL

Materials
Preparation of feedstock (BEFB)

Banana empty fruit bunch (BEFB; Bangladesh Scientific Institute of Research (BCSIR), Dhaka, Bangladesh) was used as the primary biomass feedstock. BEFB sample was vigorously washed with hot deionized water to remove dust and dried in an oven at 80 °C for 24 h. To promote effective homogeneous mixing and stirring, the sample was crushed using a ball mill. The powdered sample was sieved to remove large particles, washed, dried, and stored in a sealed container for further processing.

Preparation of hydrochar (BEFBC)

To prepare hydrochar, 5.0 g of residues was mixed with 50 mL of deionized water and stirred until it was homogeneously mixed. The sample was transferred into a Teflon-lined autoclave (100 mL) and carbonized for 12 h at 220 °C. The resulting char sample (BEFBC) was washed several times with deionized water until a neutral pH was obtained. The obtained BEFBC was not initially activated and was stored in air-tight containers for preliminary characterization studies.

Preparation of activated carbon (BEFBAC)

BEFBC (20 g) was impregnated with H_3PO_4 (100 mL, variable concentration) at 90 to 100 °C for 4 h. The sample was dried completely overnight at 90 °C. The dried sample was further pyrolyzed to enhance the surface area of the final product. The secondary stage of pyrolysis was carried out in the presence of nitrogen gas flow at varying temperatures, based on the basic design matrix (Tables 1 and 2).

Table 1. Independent Variables for Box Behnken Design

Variables	Code	Coded Variable Levels		
		-1	**0**	**+1**
Temperature (°C)	x_1	500	650	800
Carbonization Time (h)	x_2	1	2	3
H_3PO_4 Concentration (%)	x_3	25	37.5	50

The activated carbon samples (BEFBAC) were washed vigorously to remove unreacted acid. The final samples were dried and stored for further characterization.

Methods
Isotherm and thermodynamic characterization for the single solute system

Pb(II) and Zn(II) ions were prepared by dissolving $Pb(NO_3)_2.2H_2O$ or $ZnCl_2·2H_2O$ salts in de-ionized water to a final concentration of 1000 mg/L. A batch adsorption test was carried out by varying the concentration from 150, 200, 250, 300 and 350 mg/L, where the concentration gap was kept at 50 mg/L for each sample. The stock solution was further diluted to obtain the required concentration for isotherm studies. To calculate the removal percentage, the highest solution concentration of 350 mg/L was used. Adsorption experiments were carried out at 30, 60, and 80 °C for thermodynamic

characterization of the equilibrium system. The loading of Pb(II) and Zn(II) ions onto the BEFBAC was calculated using Eq. 1 (Chowdhury *et al.* 2011a, 2014),

$$q_e = \frac{(C_0 - C_e)V}{W} \tag{1}$$

where q_e represents the amount of ion adsorbed at equilibrium (mg/g), C_0 is the initial concentration of the targeted cation (mg/L), C_e is the liquid-phase concentrations of metal ions at equilibrium conditions (mg/L), V is the volume of the single solute solution (L), and W is the mass of BEFBAC used (g). For calculating the removal percentages at different experimental conditions (Table 2), the following equation was used:

$$\% \ Removal = \frac{C_0 - C_e}{C_0} \times 100 \tag{2}$$

Experimental design

The RSM technique was used to examine the impact of the major operating factors on Pb(II) and Zn(II) cation removal. The number of experiments (N) required for the BBD design is expressed by Eq. 3,

$$N = 2k \ (k - 1) + C_0 \tag{3}$$

where k is number of factors and C_0 is the number of central points. The method is less time consuming as a lower number of experimental runs is needed, when k is not too large (Ferreira *et al.* 2007). The Box Behnken Design (BBD) with three factors, including five replicates at the center point for appraisal of errors, was used to estimate the main and interaction effects of the variables and to develop a second-order polynomial model with linear, interaction, and quadratic terms. For equilibrium adsorption studies, three important effective parameters—temperature (x_1), time (x_2), and activating agent concentration (x_3)—were the independent variables, while Pb(II) removal (Y_1), Zn(II) (Y_2) removal, and carbon yield (Y_3) were the response variables (dependent variables). The variations were as follows: temperature, 500 to 800 °C; time, 1 to 3 h; and concentration of acid, 25 to 50%. The low, middle, and high levels of each variable were indicated as -1, 0, and +1, respectively. The order of the experimental runs was randomized, and the responses were used to develop empirical models using a second-degree polynomial equation (Gunaraj and Murugan 1999) Eq. 4,

$$Y = b_0 + \sum_{i=1}^{n} b_i \, x_i + \sum_{i=1}^{n} b_{ii} \, x_i^2 + \sum_{i=1}^{n} \sum_{j>1}^{n} b_{ij} \, x_i \, x_j \tag{4}$$

where Y is the predicted response, b_0 is the constant coefficient, b_i is the linear coefficient, b_{ij} is the interaction coefficients, b_{ii} is the quadratic coefficient, and x_i, and x_j are the coded values of adsorption. For the three variables, the suggested number of experiments at the center point was five, and the total number of experiments (N) required was 17 (Table 2). Table 2 summarizes the coded and actual levels of the three independent variables together with the responses obtained from the BBD experimental run represented by the design matrix.

Characterization

Surface morphological changes in the BEFB, BEFBC, and BEFBAC were characterized using field emission scanning electron microscopy (FE-SEM; model SUPRA 35VP, Zeiss, Germany, UK). The Brunauer-Emmett-Teller (BET) surface area,

micropore volume, mesopore volume, and pore size distribution of the samples were analyzed using a TriStar II BET Surface Area Analyzer (Micromeritics, USA). Prior to the nitrogen gas adsorption procedure, the samples were outgassed under a vacuum at 300 °C for 4 h to remove excess moisture content. The surface area and pore diameter were calculated using the BET method, whereas the micropore volume was obtained through the t-plot method (Storck *et al.* 1998). Carbon, hydrogen, and nitrogen contents were determined using an Elemental Analyzer (Series II 2400, PerkinElmer Inc., Japan).

RESULTS AND DISCUSSION

Development of the Regression Model

Linear, interactive, quadratic, and cubic functions were applied to the analytical data for ion removal and yield to develop regression equations. To check the adequacy of the models, three different tests were used: sequential model sum of squares, lack of fit, and model summary statistics. A cubic model was not suggested for the removal percentage and yield because of insufficient points for the calculation of the coefficients. Based on the sequential model sum of the squares and model summary statistics models, the quadratic model showed the best fit with the experimental data, having the lowest standard deviation and the highest correlation coefficient and adjusted R2 values, including the lowest P-value for Pb(II) and Zn(II) removal. A linear model was chosen for the carbon yield calculation. The experimental data were used for developing the models shown in Eqs. 5 through 7.

$$Y_1 = +80.99 + 4.97x_1 + 0.65x_2 - 3.74x_3 - 4.97x_1 x_2 - 0.76x_1 x_3 - 0.50x_2 x_3 - 9.61x_1^2 \quad (5)$$
$$-9.20x_2^2 - 3.70x_3^2$$

$$Y_2 = +63.71 - 3.01x_1 + 1.11x_2 - 0.89x_3 - 2.39x_1 x_2 - 4.00x_1 x_3 - 0.56x_2 x_3 - 8.58x_1^2 \quad (6)$$
$$-5.19x_2^2 + 1.25x_3^2$$

$$Y_3 = +36.43 - 9.25x_1 - 1.57x_2 - 2.57x_3 \quad (7)$$

The coefficients containing independent variables of temperature (x_1), time (x_2), and concentration of H_3PO_4 acid (x_3) denote the effects of the individual parameters on the response variables of Pb(II) removal (Y_1), Zn(II) removal (Y_2), and carbon yield (Y_3). Multiplication values between the two factors and others with second order terms exhibited the interaction and quadratic effect, respectively (Chowdhury *et al.* 2011b; Arami-Niya *et al.* 2012). A positive sign in front of the constant terms indicates a synergistic effect, whereas a negative sign indicates an antagonistic effect (Montgomery 2001). Figures 1(a), 1(b), and 1(c) show the experimental data versus the predicted values. The high values of the regression coefficient for all response variables indicated that the model predictions fit reasonably well with the experimental observations (Table 3).

Table 2. Experimental Responses from the Preparation of Banana Empty Fruit Bunch Activated Carbon (BEFBAC)

| Sample ID	Run	Type of Point	Reaction Variables (Actual Factors)			Lead Removal (%)	Zinc Removal (%)	Carbon Yield (%)
			Temperature, x_1 (°C)	Time, x_2 (h)	Concentration, x_3 (%)	Y_1	Y_2	Y_3
B-1	1	Center	650	2	37.50	80.88	63.88	36.66
B-2	2	Center	650	2	37.50	82.77	63.55	36.88
B-3	10	Center	650	2	37.50	79.77	63.23	37.76
B-4	11	Center	650	2	37.50	80.99	63.88	38.99
B-5	17	Center	650	2	37.50	80.56	63.99	37.88
B-6	3	IBFact	500	1	37.50	53.66	49.66	47.88
B-7	4	IBFact	650	1	25.00	68.77	57.77	39.99
B-8	5	IBFact	650	3	50.00	66.43	60.66	33.66
B-9	6	IBFact	500	3	37.50	61.44	55.88	44.67
B10	7	IBFact	650	1	50.00	62.66	58.77	31.66
B11	8	IBFact	800	3	37.50	60.77	45.44	22.66
B-12	9	IBFact	500	2	50.00	59.22	61.88	42.66
B-13	12	IBFact	800	2	25.00	77.67	58.88	30.66
B-14	13	IBFact	800	1	37.50	72.88	48.77	29.88
B-15	14	IBFact	500	2	25.00	65.54	57.32	46.77
B-16	15	IBFact	800	2	50.00	68.33	47.44	24.77
B-17	16	IBFact	650	3	25.00	74.54	61.88	35.88
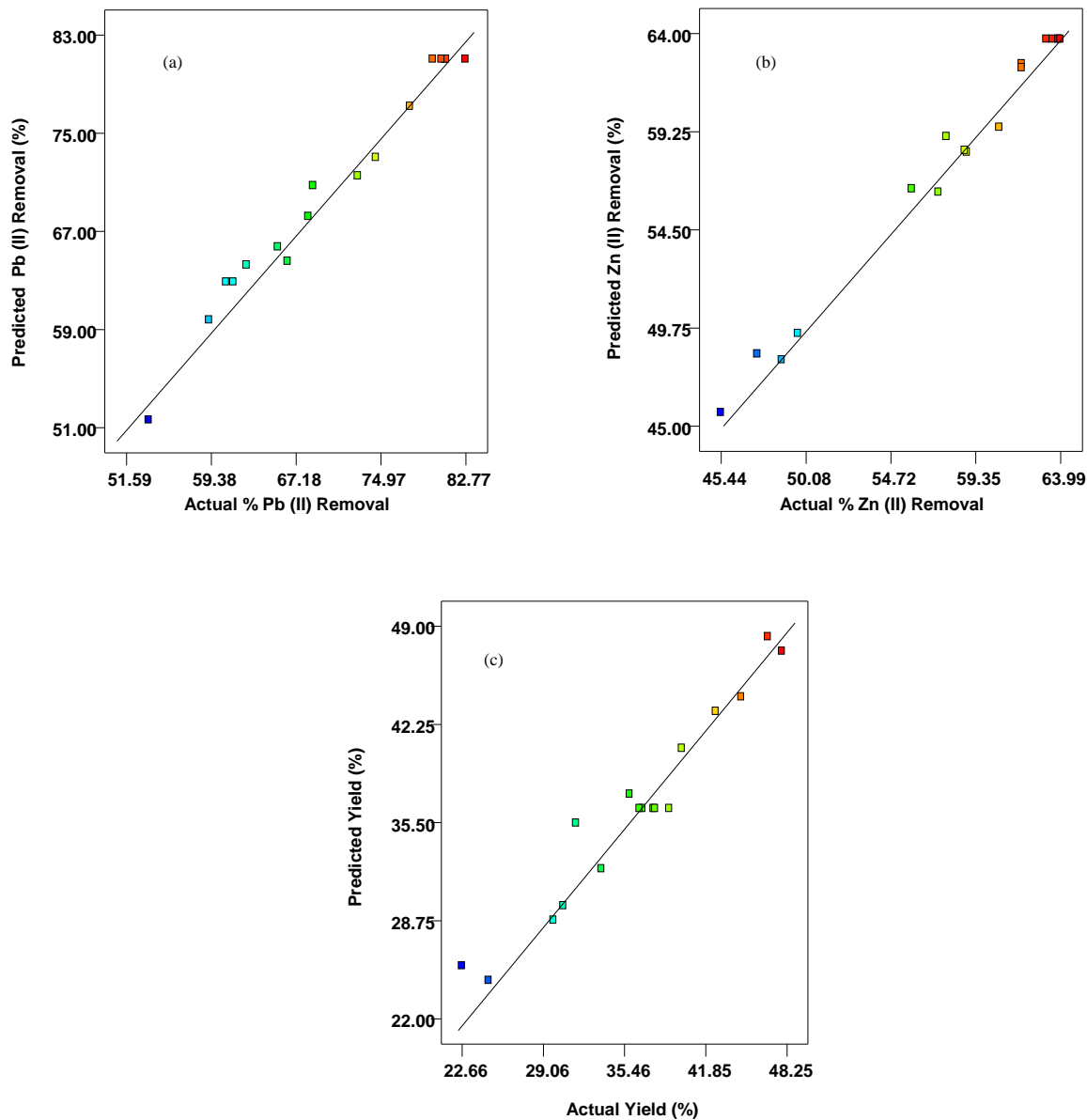
Fig. 1. Predicted versus actual (a) % removal, of Pb (II), Y_1 (b) % removal of Zn(II), Y_2 and (c) % yield of BEFBAC, Y_3

For further assessment, studentized residuals were plotted versus experimental runs for all of the responses. The experimental points for residuals were randomly scattered around zero (Fig. 2). Most of the standard residuals fell within the interval range of ± 3.00, which indicated that no response transformation was needed for the experimental design.
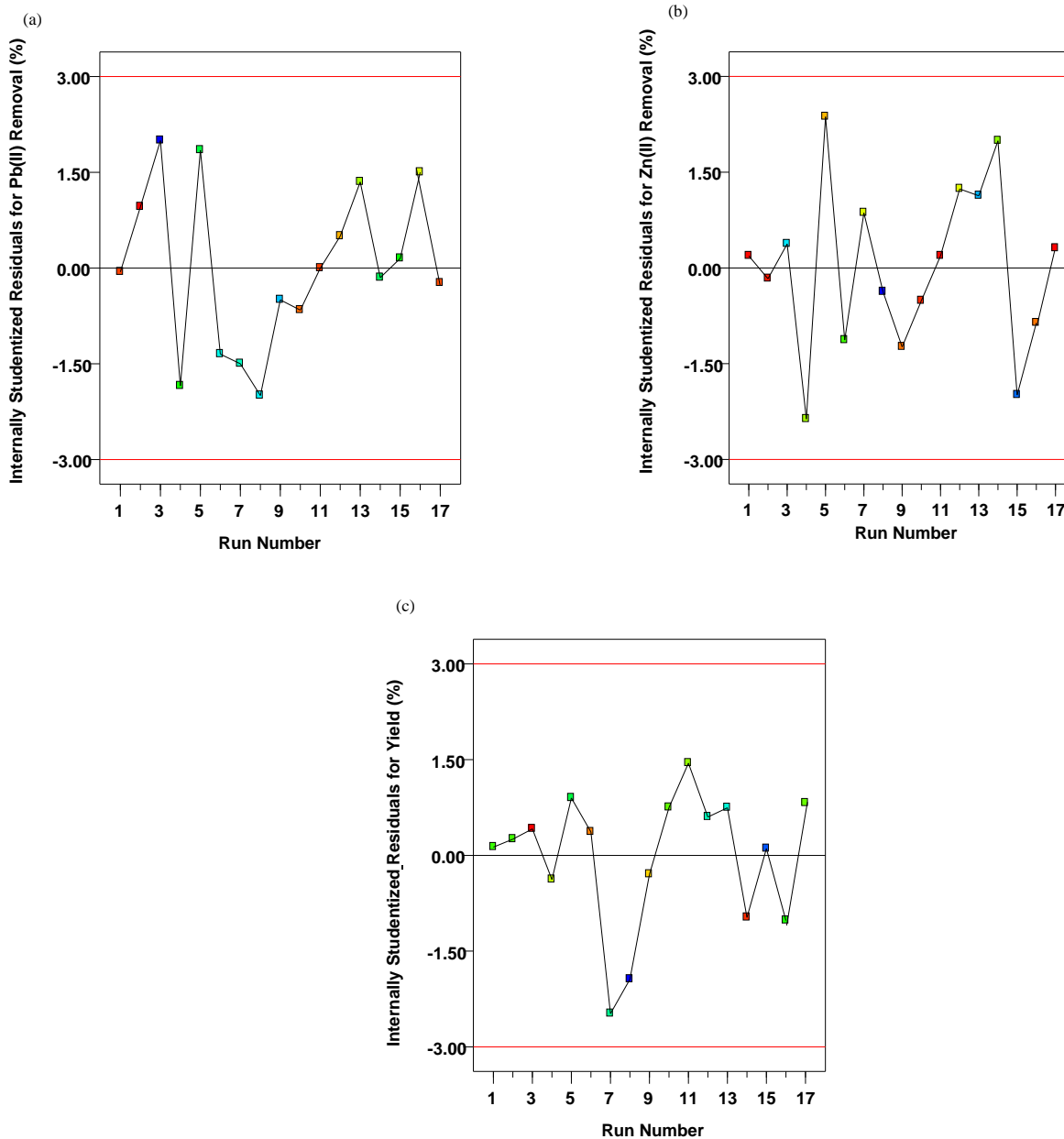
Fig. 2. Studentized residuals versus experimental run (a) % removal, of Pb(II), Y_1 (b) % removal of Zn(II), Y_2 and (c) % yield of BEFBAC, Y_3

Standard deviation was calculated to validate the quality of the models (Table 3). The experimental R^2 values were in reasonable agreement with the adjusted R^2. The values obtained for the coefficient of variation (CV) and standard deviation were small, suggesting reproducibility of the developed models. The values of adequate precision were calculated based on the signal-to-noise ratio. For effective model simulation, adequate precision should be greater than 4; the adequate precision observed for Pb(II) removal, Zn(II) removal, and carbon yield were 18.49, 22.81, and 26.65, respectively. Thus, the experimental data was statistically significant to confirm the experimental layout of the design.

Table 3. Statistical Parameters for Model Verification

Statistical Parameters	Pb(II) Removal (%)	Zn(II) Removal (%)	Yield (%)
	Y_1	Y_2	Y_3
Standard Deviation, SD	2.07	1.03	1.83
Correlation Coefficient, R^2	0.977	0.988	0.945
Adjusted R^2	0.948	0.973	0.933
Mean	70.40	57.82	36.43
Coefficient of Variation	2.94	1.79	5.02
Adequate Precision	18.49	22.81	26.65

Statistical Analysis

Statistical analysis for the developed models for all three responses was analyzed using analysis of variance (ANOVA). The analysis results are summarized in Tables 4, 5, and 6.

Table 4. Analysis of Variance (ANOVA) and Lack of Fit Test for the Removal of Pb(II) from BEFBAC (Y_1)

Source	Sum of Squares	Degrees of Freedom	Mean Square	F Value	Prob> F
Model	1296.56	9	144.06	33.54	<0.0001*
x_1	197.91	1	197.91	46.08	0.0003
x_2	3.39	1	3.39	0.79	0.4036
x_3	11.60	1	11.60	25.98	0.0014
x_1x_2	98.90	1	98.90	23.03	0.0020
x_1x_3	2.28	1	2.28	0.53	0.4899
x_2x_3	1.00	1	1.00	0.23	0.6442
x_1^2	388.71	1	388.71	90.50	<0.0001
x_2^2	356.24	1	356.24	82.94	<0.0001
x_3^2	57.51	1	57.51	13.39	0.0081
Residuals	30.06	7	4.29		
Lack of Fit	25.21	3	8.40	6.93	0.0462*
Pure Error	4.85	4	1.21		

*, significant

Based on model F-values, it can be concluded that temperature (x_1) had the greatest influence on the response of removal percentage of Pb(II) cations, Y_1, time (x_2), and ratio (x_3) had moderate influences on the removal percentage (Table 4). However, between time and H_3PO_4 concentration, the concentration of H_3PO_4 acid played vital role to enhance the quality of the prepared activated carbon. The interaction influences of temperature and time (x_1x_2) was more prominent than the other interaction factor associated with the percentage removal of Pb(II) cation, Y_1. In this case, x_1, x_3, the quadratic terms of x_1^2, x_2^2, x_3^2 including interaction terms of x_1x_2 are significant model terms (Table 4).

Table 5. Analysis of Variance (ANOVA) and Lack of Fit test for the Removal of Zn(II) from BEFBAC (Y_2)

Source	Sum of Squares	Degrees of Freedom	Mean Square	F-Value	Prob> F
Model	622.71	9	69.19	64.87	<0.0001*
x_1	73.33	1	73.33	68.75	<0.0001
x_2	9.88	1	9.88	9.26	0.0188
x_3	6.32	1	6.32	5.92	0.0452
x_1x_2	22.80	1	22.80	21.38	0.0024
x_1x_3	63.92	1	63.92	59.93	0.0001
x_2x_3	1.23	1	1.23	1.16	0.0181
x_1^2	309.82	1	309.82	290.46	<0.0001
x_2^2	113.44	1	113.44	106.35	<0.0001
x_3^2	6.63	1	6.63	6.29	0.0414
Residuals	7.47	7	1.07		
Lack of Fit	7.07	3	2.36	24.05	0.0051[*]
Pure Error	0.39	4	0.098		

* significant

For Zn(II) removal percentage, Y_2, temperature (x_1) and time (x_2) had larger influence than ratio (x_3), whereas the cumulative effect of temperature and ratio (x_1x_3) had greatest impact on removal percentages. In this case, x_1, x_2, x_3, the quadratic terms of x_1^2, x_2^2, x_3^2 including interaction terms of x_1x_2 and x_1x_3 were significant model terms (Table 5)

For yield percentage (Y_3), x_1, x_2 and x_3 were significant model terms. Table 6 reveals that temperature (x_1) and H_3PO_4 acid concentration (x_3) had more dominating effect for yield calculation. The F-test values representing the variation in the data about the mean were determined to check the competence of the models. Based on a 95% confidence interval, the model F-values for Pb(II) removal, Zn(II) removal, and carbon yield were 33.54, 64.87, and 73.52, respectively, which implied that these models were significant. However, the *P*-values for all three responses were less than 0.05, which indicated that the model terms considered for the response analysis were significant.

Table 6. Analysis of Variance (ANOVA) and Lack of Fit test for the Percent Yield of BEFBAC (Y_3)

Source	Sum of Squares	Degrees of Freedom	Mean Square	F-Value	Prob> F
Model	757.13	3	252.38	73.52	<0.0001*
x_1	684.69	1	684.69	204.88	<0.0001
x_2	19.66	1	19.66	5.88	0.0306
x_3	52.79	1	52.79	15.80	0.0016
Residuals	43.45	13	3.34		
Lack of Fit	40.01	9	4.45	0.26	5.18
Pure Error	3.43	4	0.86		

Effect of Process Parameters on Removal Percentages

Figure 3(a) demonstrates the three-dimensional response surface plots of the collective impact of temperature (x_1) and time (x_2) on the removal of Pb(II) cations (Y_1) by BEFBAC, when the H_3PO_4 concentration (x_3) was fixed at the center point (37.50%). Figure 3(b) displays the influence of temperature (x_1) and H_3PO_4 acid concentration (x_3) on the removal of Pb(II) cations, when the activation time for the hydrochar BEFBC was kept at the center point (2 h). Figures 4(a) and 4(b) are constructed to reveal the interaction of temperature and time or temperature and concentration on the removal of Zn(II) cations (Y_2) by BEFBAC. In both cases, the third variable was fixed at the center point.
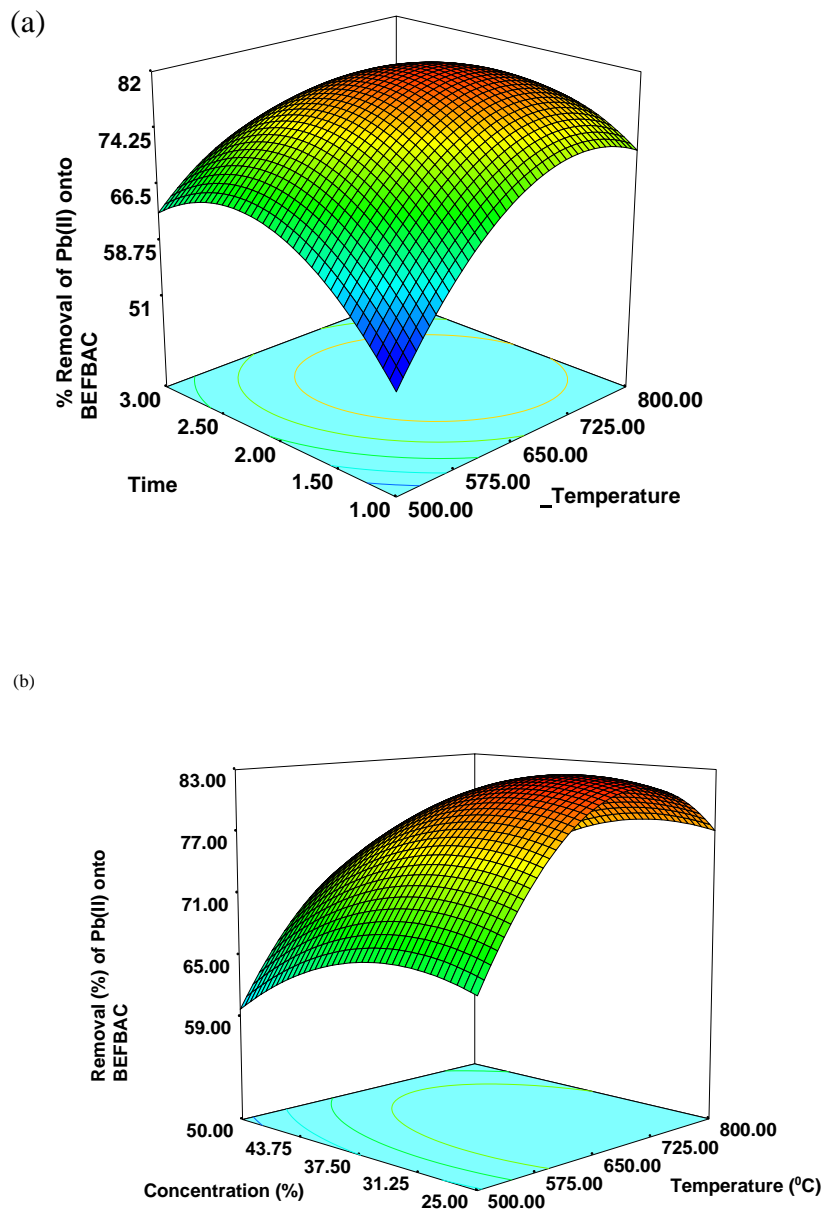
(a)

(b)

Fig. 3. Three dimensional response surface contour plots of the combined effects of (a) temperature (x_1) and time (x_2) and (b) temperature (x_1) and H_3PO_4 acid concentration (x_3) on the percent removal of Pb(II) cations by BEFBAC (Y_1), when the third variable was fixed at the center point
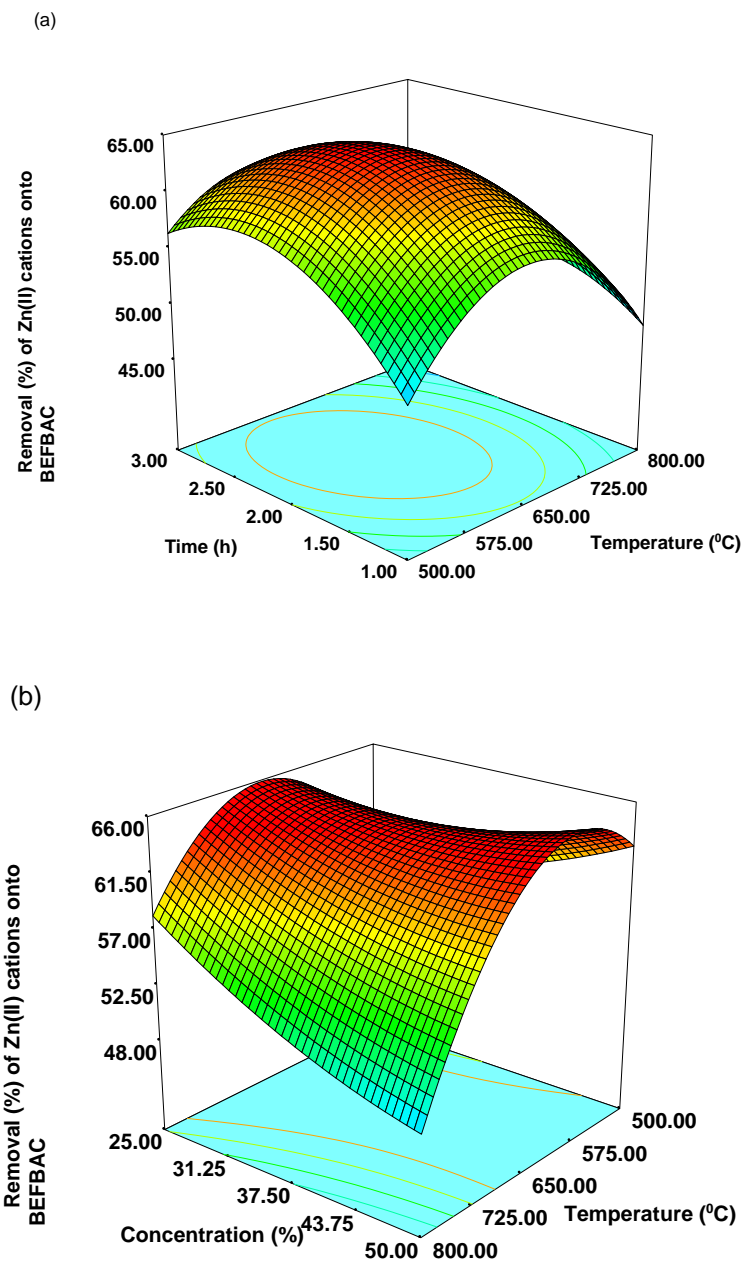
(a)

(b)

Fig. 4. Three-dimensional response surface contour plots of the combined effects of (a) temperature (x_1) and time (x_2) and (b) temperature (x_1) and H_3PO_4 acid concentration (x_3) on the percent removal of Zn(II) cations by BEFBAC (Y_2), when the third variable was fixed at the center point

The curvature observed in Figs. 3 and 4 represents the prominent effect of the activation temperature on the removal of both cations, irrespective of the time and concentration of H_3PO_4. The plots revealed that the temperature and concentration of the impregnating acid was proportional to the percentage removal. Up to a certain limit, increasing of temperature and acid concentration enhanced the reaction, resulting in more

surface area with a porous texture, which is desirable for adsorption. ANOVA also showed that the activation temperature had the highest impact on ion removal. In previous studies, the activation time exhibited a moderate to minimal impact on the development of the surface area and pore structure of the activated carbon prepared from cassava peel, whereas the pore distribution in terms of micropore and mesopore percentages were strongly influenced by the activating KOH impregnation ratio and the temperature (Sudaryanto *et al.* 2006). A short activation time and very low temperature might not be sufficient to enhance the surface area (Cao *et al.* 2006). After a certain limit, increasing the temperature and concentration both exhibited a detrimental effect on the percentage removal; high temperature or acid concentration might destroy some surface functional groups. In addition, these conditions might compromise the integrity of the porous texture of AC by thermal annealing, which destroys the walls of the micropores to form more mesopores, which are suitable for liquid phase adsorption. However, in that case, the pore size distribution is not suitable, because larger mesopores fail to adsorb and retain smaller cations, resulting in lower removal efficiency (Chowdhury *et al.* 2012). At very high temperatures and longer residence times with highly concentrated acid, the carbon skeleton might burn into ash, which also compromises removal efficiency. A very long activation time is not beneficial, as it increases the liquid yield and reduces the carbon yield, with successive decreases in the removal efficiency. This trend was also observed during the preparation of activated carbon from oil palm fronds for the removal of Zn(II) cations (Zahangir *et al.* 2008).

Effect of Process Parameters on Carbon Yield

Figure 5a reveals the cumulative influence of two independent factors, temperature and time, on percentage yield of carbon when the H_3PO_4 concentration was fixed at the center point (37.50%). Figure 5b shows the combined impact of temperature and H_3PO_4 concentration over yield percentage, where time was kept at the center point of 2 h. All three parameters exhibited a synergistic effect on percentage yield.

In general, the yield decreased with increasing temperature, time, and acid concentration. Temperature had the highest impact on the yield percentage, which was earlier shown by the highest F-value of 684.69 (Table 6), whereas the activation time was not as noteworthy compared to the temperature and acid concentration. Temperature was the dominant factor relative to the yield, as supported by the ANOVA data (Table 6). The lowest yield was obtained at 800 °C for 3 h with 37.50% acid (Sample B-11, Table 2). With increased temperature, the contact time and concentration intensified the diffusion of acidic solution inside the hydrochar matrix, leading to conversion of carbon to ash. This effect initiated the disintegration of the crystalline region of hydrochar and formed amorphous carbon, which is desirable for adsorbent preparation. Thus, the optimum reaction condition should be determined to enhance the surface area of the carbon sample with the highest possible yield. Consequently, the removal efficiency would also be higher.

This observation is consistent with the previous work on cassava peel (Sudaryanto *et al.* 2006), where activation temperature was the most important factor, role, and activation time had the least impact on the carbon yield. Increasing the temperature beyond a certain point enhanced dehydration and elimination reactions to release additional volatile organic fractions from the hydrochar matrix as gaseous and aqueous products, rather than as solid activated carbon.
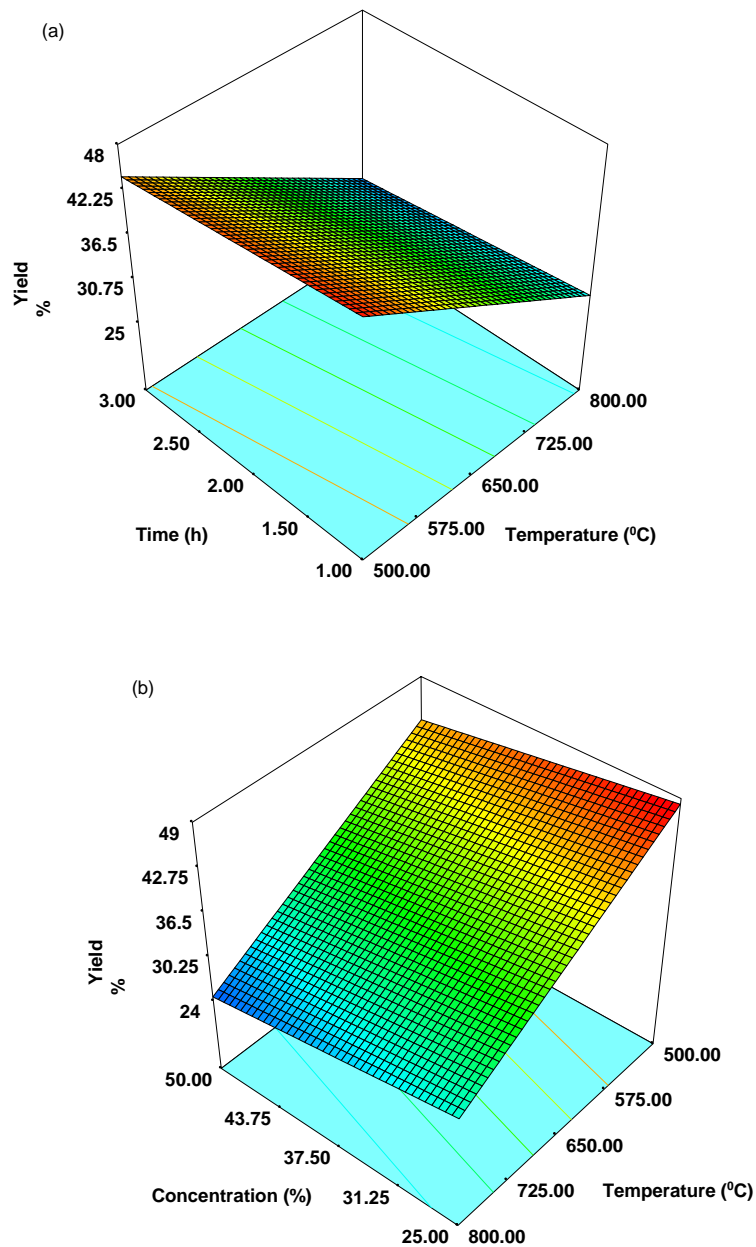
Fig. 5. Three-dimensional response surface contour plots of the combined effects of (a) temperature (x_1) and time (x_2) and (b) temperature (x_1) and H$_3$PO$_4$ acid concentration (x_3) on the percent yield of BEFBAC (Y_2), when the third variable was fixed at the center point

Model Validation and Confirmation

For the robustness of experimental design to manufacture carbon, relatively high removal efficiencies, along with satisfactory carbon yields were expected for targeting pollutants under optimum conditions. When the independent variables of temperature, time, and acid concentration were increased, the percentage removal increased up to a certain point, whereas the yield decreased. The converse effects were also observed. To optimize the char activation process, maximum values for removal were set as the targets,

while the three variables (temperature, time, and acid concentration) were set within the studied ranges. A 1.0-g sample was used as the input for each parameter to control the desirability function (Amini *et al.* 2008). The desirability function for optimization and error percentage were estimated (Table 7).

Characterization

The obtained hydrochar was brown in color and consistent with partially carbonized products. SEM images of the raw lignocellulosic residues (BEFB) showed a smooth, nonporous texture without cracks (Fig. 6a), but after carbonization (BEFBC and BEFBAC), there were substantial changes in the surface morphology and texture. Many sphere-like microparticles were deposited over the larger particles (BEFBC). Cellulose and hemicellulose were degraded during hydrothermal carbonization, producing carbon microspheres (Liu and Guo 2015). However, the more chemically stable non-saccharide components of biomass (lignin) were only partially degraded, which preserved the original skeleton of the particles (Sevilla and Fuertes 2009; Gao *et al.* 2012; Falco *et al.* 2013). After activation, BEFBAC particle surfaces were characterized by large conchoidal cavities with smooth surface structures (Fig. 6c). Thus, acid activation caused drastic morphological changes, as previously reported for eucalyptus wood-based hydrochar (Sevilla and Fuertes 2011).
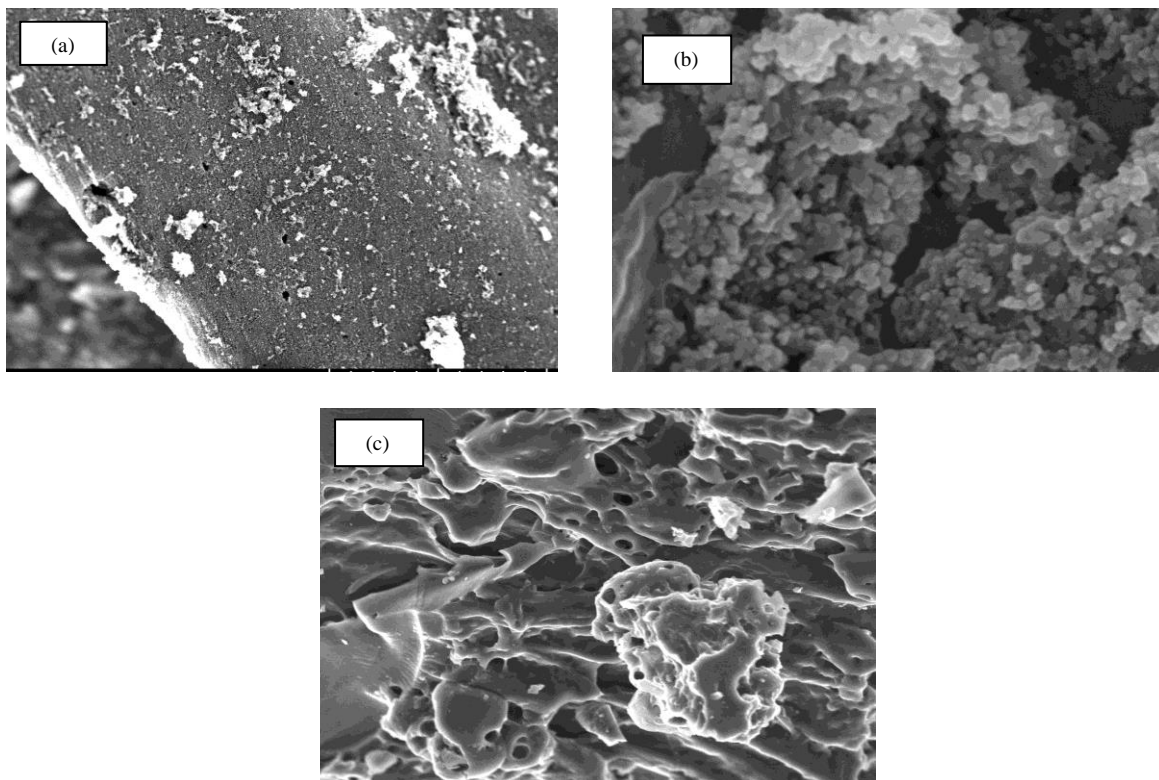

Fig. 6. SEM images of (a) banana empty fruit bunch (BEFB), (b) hydrochar (BEFBC), and (c) hydrochar activated carbon (BEFBAC)

bioresources.com

Table 7. Process Parameter Optimization for BEFBAC

Temperature (x₁)	Time (x₂)	Concentration (x₃)	Percentage Removal Pb(II) (Y₁)			Percentage Removal Zn(II) (Y₂)			Percentage Yield (Y₃)			Desirability
(°C)	(h)	(%)	Predicted	Experimental	Error	Predicted	Experimental	Error	Predicted	Experimental	Error	-
599.45	2.04	25.97	78.39	82.85	5.68	64.49	61.02	5.38	41.45	42.76	3.16	0.87

bioresources.com

The XRD patterns of BEFB, along with hydrochar (BEFBC) and activated carbon (BEFBAC), obtained in the 2θ range of 10 to 35° are shown in Fig. 7. Sharp peaks were observed around 16° and 22° for the original biomass (BEFB) and hydrochar (BEFBC), indicating crystalline regions of cellulose (Keiluweit *et al.* 2010). The biomass and the hydrochar samples showed similar XRD patterns, reflecting that the hydrothermal carbonization did not disrupt crystalline cellulose.

After activation, the peak intensity became lower and broader, reflecting a decrease in crystallinity. Therefore, the carbon content present in hydrochar-based activated carbon (BEFBAC) was mainly amorphous in texture. This result was expected, as amorphous materials show better absorbance due to their high surface area and greater number of active sites (Tchomgui-Kamga *et al.* 2010). Previous findings also demonstrated the presence of amorphous carbon in coconut coir-based activated carbon (Sharma and Gode 2010).
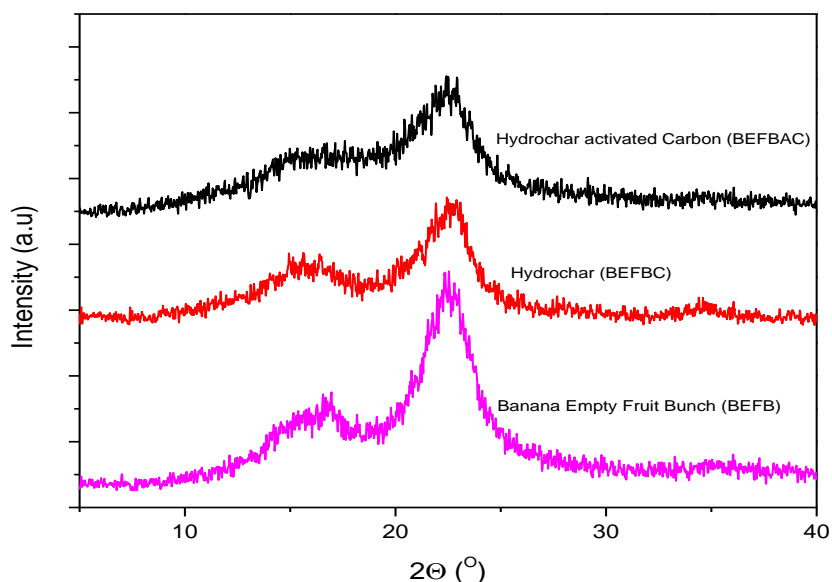

Fig. 7. XRD pattern of banana empty fruit bunch (BEFB), hydrochar (BEFBC), and hydrochar activated carbon (BEFBAC)

The texture of hydrochar (BEFBC) and hydrochar carbon (BEFBAC) were analyzed by means of nitrogen physi-sorption (Table 8). The BEFBC sample exhibited less surface area with poor porosity, which was attributed to incomplete carbonization. Thus, the obtained hydrochar material obtained virtually no framework of confined pores. Its surface area arises only from inter-particle voids (Sun *et al.* 2015).

The biomass type and temperature play a vital role in hydrochar surface area by controlling the amount of pores by cracking the basal structural sheets of hydrochar (Novak *et al.* 2009; Mumme *et al*. 2011). After chemical activation with H_3PO_4, the surface area and pore volume increased substantially. The reaction between H_3PO_4 and hydrochar structural compounds led to further depolymerization, which enhanced pore volume (Fernandez *et al*. 2015).

Table 8. Physico-Chemical Characteristics of BEFBC and Activated BEFBAC

Sample Properties	BEFBC	BEFBAC
BET surface area (m^2/g)	7.01	762.05
Micropore surface area (m^2/g)	1.01	1004.30
Total pore volume (cc/g)	0.1003	0.4321
Average pore diameter (°A)	1.01	18.22
BJH cumulative adsorption surface area (m^2/g)	2.62	522.72

Table 9 lists the ultimate analysis of biomass, hydrochar, and hydrochar activated carbon. After hydrothermal carbonization, the carbon content of the char increased, whereas the hydrogen and oxygen contents decreased (Saqib *et al.* 2015). After activation, the carbon content increased substantially. Both the H/C and O/C ratios decreased after carbonization and activation. The H/C ratio decreased due to aromatization that occurred during hydrothermal carbonization. The O/C ratio decreased as a result of decarboxylation, whereas both the H/C and O/C ratios decreased *via* dehydration (Liu and Guo 2015).

Table 9. Ultimate Analysis of BEFB, BEFBC, and BEFBAC

Ultimate Analysis	BEFB	BEFBC	BEFBAC
Carbon (%)	42.09	52.55	81.55
Hydrogen (%)	5.99	4.56	3.51
Nitrogen (%)	1.33	1.00	1.02
Oxygen (%)	47.00	39.13	12.91
Others (%)	3.59	2.76	1.01
H/C	0.142	0.086	0.043
O/C	1.11	0.744	0.158

Equilibrium Isotherm Studies

Isotherm parameters were evaluated using three types of linear model equations, namely Langmuir, Freundlich, and Temkin. Results are listed in Table 11. Maximum monolayer adsorption capacity, q_m (mg/g), and Langmuir's constant, K_L (L/mg), demonstrated the binding energy for adsorption uptake under optimum conditions, as determined from Langmuir's model in Eq. 8 (Langmuir 1918):

$$q_e = \frac{K_L C_e}{1 + K_L C_e} \tag{8}$$

Equation 8 was linearized to give Eq. 9:

$$\frac{C_e}{q_e} = \frac{1}{q_{max} K_L} + \frac{1}{q_{max}} C_e \tag{9}$$

The dimensionless factor, R_L, of the Langmuir's model can be calculated using Eq. 10:

$$R_L = \frac{1}{1 + K_L C_o}$$
(10)

R_L values were calculated for the highest initial concentration (350 mg/L). The separation factor, R_L, was determined to elucidate the types of isotherms (Table 10; Chowdhury *et al.* 2015).

Table 10. Types of Isotherms Based on the Separation Factor, R_L

Value of R_L	Magnitude	Types of Isotherms
$R_L > 1$	Greater than one	Unfavorable
$R_L = 1$	Equal to one	Linear
$0 < R_L < 1$	Between zero to one	Favorable
$R_L = 0$	Zero	Irreversible

The surface heterogeneity, to show the multilayer adsorption properties of BEFBAC, can be observed using Freundlich's isotherm. The empirical equation shows that the reactive sites over the carbon sample are scattered exponentially with the heat of the adsorption process (Freundlich 1906). The nonlinear form of Freundlich's equation is given by:

$$q_e = K_f C_e^{1/n}$$
(11)

The above equation was linearized to determine the parameters (Eq. 11),

$$\ln q_e = \ln K_f + \frac{1}{n} \ln C_e$$
(12)

where K_f is the affinity factor of the cations towards the carbon sample (BEFBAC) (mg/g) and $1/n$ represents the intensity of the adsorption.

The equilibrium data were further analyzed by the Temkin isotherm and are expressed by Eq. (13) (Temkin and Pyzhev 1940):

$$q_e = \frac{RT}{b} \ln K_T C_e$$
(13)

Equation 13 can be linearized as,

$$q_e = \frac{RT}{b} \ln K_T + \frac{RT}{b} \ln C_e$$
(14)

where $RT/b = B$ denotes the Temkin constant (J/mol), which depicts the heat of the sorption process, whereas K_T reflects the equilibrium binding constant (L/g), R is the universal gas constant (8.314 J/mol·K), and $T°$ is the absolute solution temperature (K) (Temkin and Pyzhev 1940).

Table 11. Langmuir, Freundlich, and Temkin Model Parameters at Different Temperatures

Pollutant	Temperature (°C)	Langmuir Isotherm				Freundlich Isotherm			Temkin Isotherm		
		q_{max} (mg/g)	K_L (L/mg)	R^2	R_L	K_F (mg/g)(L/mg)$^{1/n}$	$1/n$	R^2	B	K_T (L/mg)	R^2
	30	74.62	0.300	0.99	0.009	33.93	0.18	0.97	23.2	9.88	0.97
Pb(II)	60	78.74	0.413	0.99	0.007	37.01	0.20	0.99	29.0	10.48	0.99
	80	79.36	0.445	0.99	0.006	38.19	0.19	0.99	35.2	10.38	0.99
	30	77.51	0.075	0.97	0.041	17.99	0.31	0.71	38.3	6.47	0.58
Zn(II)	60	76.33	0.086	0.97	0.032	19.45	0.29	0.60	1.32	14.80	0.71
	80	80.64	0.071	0.98	0.041	16.04	0.35	0.90	0.74	17.31	0.89

In this work, relatively better linearity for the Langmuir model was observed for Pb(II) and Zn(II) cations at temperatures of 30, 60, and 80 °C. The Langmuir separation factor, R_L, and the Freundlich exponent, $1/n$, were below 1.0 percent for all the temperatures, suggesting a favorable adsorption processes. Similar observations for R_L and $1/n$ were reported for Mn(II) sorption onto raw- and acid-treated corncob biomass and mangostene fruit peel-based activated carbon (Abideen *et al.* 2011; Chowdhury *et al.* 2014).

Thermodynamic Characterization

The thermodynamic characterization of the equilibrium system provides the values of Gibbs free energy ($\Delta G°$), enthalpy ($\Delta H°$), and entropy ($\Delta S°$) of the sorption process. The following linear equations were used to interpret the equilibrium data (Chowdhury *et al.* 2011a),

$$\ln K_L = \frac{S}{R} - \frac{H}{RT} \tag{15}$$

$$G = RTLnK_L \tag{16}$$

where the constant, K_L was determined from the Langmuir equation at three different temperatures (L/mg; Table 11), R is the universal gas constant (8.314 J/mol·K), and T is the absolute temperature (K) (Ahmad 2006).

The thermodynamic parameters Gibbs free energy ($\Delta G°$), enthalpy ($\Delta H°$), and entropy ($\Delta S°$) were calculated (Table 12). The enthalpy ($\Delta H°$) calculated for both the cations showed a positive magnitude, indicating that the process was endothermic (Chowdhury *et al.* 2014). Thus, the removal of both cations was improved by increased temperature.

A positive value of entropy ($\Delta S°$) reflected an increase in the degrees of freedom for the equilibrium system. Similar phenomena were reported for the removal of divalent lead cations from synthetic water using activated palm ash residues (Chowdhury *et al.* 2011a). The Gibbs free energy change ($\Delta G°$) estimated for all of the temperatures was negative, indicating the feasible and spontaneous nature of sorption (Chowdhury *et al.* 2011c, d).

bioresources.com

Table 12. Thermodynamic Parameters of Pb(II) and Zn(II) Sorption by BEFBAC

Pollutant	Temperature (K)	Thermodynamic Parameters			
		$\Delta G°$ (kJ·mol^{-1})	$\Delta H°$ (kJ·mol^{-1})	$\Delta S°$ (J·K^{-1}·mol^{-1})	R^2
	303	-3.029			
Pb(II)	333	-3.062	0.1106	0.3459	0.9974
	353	-3.316			
	303	-6.497			
Zn(II)	333	-4.433	0.1347	0.7092	0.9991
	353	-4.355			

CONCLUSIONS

1. AC preparation factors were optimized using response surface methodology based on a Box Behnken Design. The activation temperature, time, and concentration of acid substantially influenced each response variable.

2. Model validation was conducted under optimum conditions. The developed models were significant enough to calculate the values of the responses reasonably well. The deviation errors between the predicted and experimental results for Pb(II) removal, Zn(II) removal, and AC yield were 5.68%, 5.38%, and 3.16%, respectively.

3. The surface area and carbon content of the prepared hydrochar were enhanced by activation

4. The equilibrium data and linear regression analysis at room temperature using Langmuir, Freundlich, and Temkin isotherms exhibited a maximum monolayer sorption capacity of 74.62 mg/g and 77.51 mg/g for Pb(II) and Zn(II) cations, respectively.

5. Equilibrium thermodynamic studies showed that the process was endothermic, spontaneous, and feasible for the temperature ranges investigated.

ACKNOWLEDGMENTS

REFERENCES CITED

Abideen, I. A., Ofudje, A. E., Mopelola, A. I., and Sarafadeen, O. K. (2011). "Equilibrium kinetics and thermodynamics studies of the biosorption of Mn(II) ions from aqueous solution by raw and acid treated corn cob biomass," *BioResources* 6(4), 4117-4134. DOI: 10.15376/biores.6.4.4117-4134

Ahmad, A. A. (2006). *Isotherm, Kinetics and Thermodynamic Studies of Dyes Adsorption from Aqueous Solution onto Activated Palm Ash and Bentonite*, M.S. thesis,

University Science Malaysia, Pulau Penang, Malaysia.

Amaya, A., Medero, N., Tancredi, N. H., Silva, H., and Deiana, C. (2007). "Activated carbon briquettes from biomass materials," *Bioresour. Technol.* 98(8), 1635-1641. DOI: 10.1016/j.biotech.2006.05.049

Amini, M., Habibullah, Y., Nader, B., Ali Akbar, Z. L., Farshid, G., Ali, D., and Mazyar, S. (2008). "Application of response surface methodology for optimization of lead biosorption in an aqueous solution by *Aspergillus*," *J. Hazard. Mater.* 154, 694-702. DOI: 10.1016/j.jhazmat.2007.10.114

Arami-Niya, A., Faisal, A., Mohammad, S. S., Wan Daud, W. M. A., and Sahu, J. N. (2012). "Optimization of synthesis and characterization of palm shell based bio-chars as a by-product of bio-oil production process," *BioResources* 7(1), 246-264. DOI: 10.15376/biores.7.1.246-264

Baskan, M. B., and Pala, A. (2010). "A statistical experiment design approach for arsenic removal by coagulation process using aluminum sulfate," *Desalination* 254(1-3), 42-48. DOI: 10.1016/.j.desal.2009.12.106S

Cao, Q., Xie, K. C., Lv, Y. K., and Bao, W. R. (2006). "Process effects on activated carbon with large specific surface area from corn cob," *Bioresour. Technol.* 97(1), 110-115. DOI: 10.1016/j.biortech.2005.02.026

Chowdhury, Z. Z., Zain, S. M., and Rashid, A. K. (2011a). "Equilibrium isotherm modeling, kinetics, and thermodynamics study for removal of lead from waste water," *E- J. Chem.* 8(1), 333- 339. DOI: 10.1155/2011/184040

Chowdhury, Z. Z., Zain, S. M., Rashid, A. K., Ahmad, A. A., Islam, M. S., and Arami-Niya, A. (2011b). "Application of central composite design for preparation of kenaf fiber based activated carbon for adsorption of manganese (II) ion," *IJPS* 6(31), 7191-7202. DOI: 10.5897/IJPS11.1510

Chowdhury, Z. Z., Zain, S. M., Rashid, A. K., and Ahmed, A. A. (2011c). "Equilibrium kinetics and isotherm studies of Cu (II) adsorption from waste water onto alkali activated oil palm ash," *Am. J. Applied Sci.* 8(3), 230-237. DOI: 10.3844/ajassp.2011.230.237

Chowdhury, Z. Z., Zain, S. M., Rashid, A. K., and Islam, M. S. (2011d). "Preparation and characterizations of activated carbon from kenaf fiber for equilibrium adsorption studies of copper from wastewater," *KiChE* 29(9), 1187-1195, DOI: 10.1007/s11814-011-0297-9.

Chowdhury, Z. Z., Zain, S. M., Rashid, A. K., and Khalid, K. (2012). "Process variables optimization for preparation and characterization of novel adsorbent from lignocellulosic waste," *BioResources* 7(3), 3732-3754. DOI: 10.15376/biores.7.3.3732-3754

Chowdhury, Z. Z., Abd Hamid, S. B., Das, R., Hasan, H. R., Zain, S. M., Khalid, K., and Uddin, M. N. (2013). "Preparation of carbonaceous adsorbents from lignocellulosic biomass and their use in removal of contaminants from aqueous solution," *BioResources* 8(4), 6523-6555. DOI: 10.15376/biores.8.4.6523-6555

Chowdhury, Z. Z., Abd Hamid, S. B., and Zain, S. M. (2014). "Base catalytic approach: A promising technique for activation of bio char for equilibrium sorption studies of copper, Cu (II) ions in single solute system," *Materials* 7(4), 2815-2832. DOI: 10.3390/ma7042815

Chowdhury, Z. Z., Hasan, M. D., Abd Hamid, S. B., Shamsudin, E. M., Zain, S. M., and Khalid, K. (2015). "Catalytic pretreatment of biochar residues derived from lignocellulosic feedstock for equilibrium studies of manganese, Mn (II) cations from

aqueous solution," *RSC Adv.* 5(9), 6345-6356. DOI: 10.1039/C4RA09709B

Falco, C., Sieben, J. M., Brun, N., Sevilla, M., Van der Mauelen, T., Morallon, E., Cazorla-Amoros, D., and Titirici, M. M. (2013). "Hydrothermal carbons from hemicellulose-derived aqueous hydrolysis products as electrode materials for supercapacitors," *ChemSusChem* 6(2), 374-382. DOI: 10.1002/cssc.201200817

Fernandez, M. E., Ledesma, B., Román, S., Bonelli, P. R., and Cukierman, A. L. (2015). "Development and characterization of activated hydrochars from orange peels as potential adsorbents for emerging organic contaminants," *Bioresour. Technol.* 183, 221-228. DOI: 10.1016/j.biotech.2015.02.035

Ferreira, S. L. C., Bruns, R. E., Ferreira, H. S., Matos, G. D., David, J. M., Brand, G. C., da Silva, E. G. P., Portugal, L. A., dos Reis, P. S., Souza, A. S., and dos Santos, W. N. L. (2007). "Box-Behnken design: An alternative for the optimization of analytical methods," *Anal. Chim. Acta* 597(2), 179-186. DOI: 10.1016/j.aca.2007.07.011

Freundlich, H. M. F. (1906). "Over the adsorption in solution," *J. Phys. Chem.* 57(1906), 385-471.

Gao, Y., Wang, X. H., Yang, H. P., and Chen, H. P. (2012). "Characterization of products from hydrothermal treatments of cellulose," *Energy* 42(1), 457-465. DOI: 10.1016/j.energy.2012.03.023S

Gunaraj, V., and Murugan, N. (1999). "Application of response surface methodologies for predicting weld base quality in submerged arc welding of pipes," *J. Mater. Process Technol.* 88(1-3), 266-275. DOI: 10.1016/S0924-0136(98)00405-1

Hao, W., Björkman, E., Lilliestråle, M., and Hedin, N., (2014). "Activated carbons for water treatment prepared by phosphoric acid activation of hydrothermally treated beer waste," *Ind. Eng. Chem. Res.* 53, 15389-15397. DOI: 10.1021/ie5004569.

Keiluweit, M., Nico, P. S., Johnson, M. G., and Kleber, M. (2010). "Dynamic molecular structure of plant biomass-derived black carbon (biochar)," *Environ. Sci. Technol.* 44(4), 1247-1253. DOI: 10.1021/es9031419

Langmuir, I. (1918). "The adsorption of gases on plane surfaces of glass, mica and platinum," *J. Am. Chem. Soc.* 40(9), 1361-1403. DOI: 10.1021/ja02242a004

Liu, F., and Guo, M. (2015). "Comparison of the characteristics of hydrothermal carbons derived from holocellulose and crude biomass," *J. Mater. Sci.* 50(4), 1624-1631. DOI: 10.1007/s10853-014-8723-0

Montgomery, D. C. (2001). *Design and Analysis of Experiments* (5th Ed.), John Wiley and Sons, New York.

Mumme, J., Eckervogt, L., Pielert, J., Diakité, M., Rupp, F., and Kern, J. (2011). "Hydrothermal carbonization of anaerobically digested maize silage," *Bioresour. Technol.* 102(19), 9255-9260. DOI: 10.1016/j.biotech.2011.06.099

Novak, J. M., Lima, I. M., Xing, B., Gaskin, J. W., Steiner, C., Das, K. C., Ahmedna, M., Rehrah, D., Watts, D. W., Busscher, W. J., and Schomberg, H. (2009). "Characterization of designer biochar produced at different temperatures and their effects on a loamy sand," *Annals of Environ. Sci.* 3, 195-206.

Román, S., Valente Nabais, J. M., Ledesma, B., González, J. F., Laginhas, C., and Titirici, M. M. (2013). "Production of low-cost adsorbents with tunable surface chemistry by conjunction of hydrothermal carbonization and activation processes," *Micropor. Mesopor. Mater.* 165(2013), 127-133. DOI: 10.1016/j.micrmeso.2012.08.006

Saqib, U., N, Oh, M., Jo, W., Park, S., and Lee, J-Y. (2015). "Conversion of dry leaves into hydrochar through hydrothermal carbonization (HTC)," *J. Mater. Cycles Waste*

Manag. (online), DOI 10.1007/s10163-015-0371-1.

Sevilla, M., and Fuertes, A. B. (2009). "The production of carbon materials by hydrothermal carbonization of cellulose," *Carbon* 47(9), 2281-2289. DOI: 10.1016/j.carbon.2009.04.026

Sevilla, M., and Fuertes, A. B. (2011). "Sustainable porous carbons with a superior performance for CO_2 capture," *Energy Environ. Sci.* 4, 1765-1771. DOI: 10.1039/C0EE00784F

Sharma, Y., and Gode, F. (2010). "Engineering data for optimization of preparation of activated carbon from an economically viable material," *J. Chem. Eng. Data* 55(9), 3991-3994. DOI: 10.1021/je100041x

Storck, S., Bretinger, H., and Maier, W. F. (1998). "Characterization of micro- and mesoporous solids by physisorption methods and pore-size analysis," *Appl. Catal. A: General* 174(1-2), 137-146. DOI: 10.1016/S0926-860X(98)00164-1.

Sudaryanto, Y., Hartono, S. B., Irawaty, W., Hindarso, H., and Ismadji, S. (2006). "High surface area activated carbon prepared from cassava peel by chemical activation," *Bioresour. Technol.* 97(5), 734-739. DOI: 10.1016/j.biortech.2005.04.029t.

Sun, K., Tang, J., Yanyan, G., and Zhang, H. (2015). "Characterization of potassium hydroxide (KOH) modified hydrochars from different feedstocks for enhanced removal of heavy metals from water," *Environ. Sci. Pollut. Res.* 22(21), 16640-16651. DOI: 10.1007/s11356-015-4849-0

Tchomgui-Kamga, E., Alonzo, V., Nanseu-Njiki, C. P., Audebrand, N., Ngameni, E., and Darchen, A. (2010). "Preparation and characterization of charcoals that contain dispersed aluminum oxide as adsorbents for removal of fluoride from drinking water," *Carbon* 48(2), 333-343. DOI: 10.1016/j.carbon.2009.09.034

Temkin, M. J., and Pyzhev, V. (1940). "Recent modification to Langmuir isotherms," *Acta Phys. Chem.* 12, 217-225.

Titirici, M. M., Thomas, A., and Antonietti, A. (2007a). "Back in the black: Hydrothermal carbonization of plant material as an efficient chemical process to treat the CO_2 problem?" *New J. Chem.* 6(2007), 787-789. DOI: 10.1039/B616045J

Titirici, M. M., Thomas, A., Yu, S. H., Müller, J. O, and Antonietti, A. (2007b). "A direct synthesis of mesoporous carbons with bicontinuous pore morphology from crude plant material by hydrothermal carbonization," *Chem. Mater.* 19(17), 4205-4212. DOI: 10.1021/cm0707408

Titirici, M. M., Antonietti, M., and Baccile, N. (2008). "Hydrothermal carbon from biomass: A comparison of the local structure from poly- to monosaccharides and pentoses/hexoses," *Green Chem.* 10(11), 1204-1212. DOI: 10.1039/B807009A

Xiu, S., Shabazi, A., Shirley, V., and Cheng, D. (2010). "Hydrothermal pyrolysis of swine manure to bio-oil: Effects of operating parameters on products yield and characterization of bio-oil," *J. Anal. Appl. Pyrolysis* 88(1), 73-79. DOI: 10.1016/j.jaap.2010.02.011

Zahangir, M. A., Suleyman, A. M., and Noraini, K. (2008). "Production of activated carbon from oil palm empty fruit bunches for removal of zinc," in: *Twelfth International Water Technology Conference*, Alexandria, Egypt, pp. 373-383.